NUMERICAL SOLUTION OF THE WATERHAMMER EQUATIONS USING THE METHOD OF CHARACTERISTICS AND COMPARISON AGAINST EXPERIMENTS

Ajit P. Muzumdar

Nuclear Safety Analysis Department
Ontario Hydro, 700 University Avenue
Toronto, Ontario M5G 1X6

ABSTRACT

This paper describes the development and application of a mathematical model and numerical solution method for the transient flow behaviour of a fluid in a system of pipes. The type of problem studied falls under classical waterhammer theory, and the solution technique is the method of characteristics.

This method is applied in a computer program WHAM which was initially developed to model a series of waterhammer experiments simulating the rupture of a pressure tube within a CANDU nuclear reactor. The WHAM code was then modified considerably to model the acoustic response of a general piping network.

Application of the WHAM code to various experiments is discussed.

INTRODUCTION

This paper describes the development and application of a mathematical model and numerical solution method for the transient flow behaviour of a fluid in a system of pipes. The type of problem studied falls under classical waterhammer theory, and the solution technique is the method of characteristics.

This method is applied in a computer program WHAM which was initially developed to model a series of waterhammer experiments simulating the rupture of a pressure tube within a CANDU nuclear reactor (Reference 1). The WHAM code was then modified considerably to model the acoustic response of a general piping network, with particular application to a single core pass of the Darlington reactor, from the pump discharge, to the RIH, and through each of the 120 channels to the ROH. Other connecting pipes such as the ECI and SDC pipes are also included in the model.

An important input to the code is the pressure wave or sonic velocity in various parts of the piping network. The method used to obtain this velocity is briefly reviewed, including such effects as pipe elasticity, and in the case of the pressure tube rupture experiments, non-condensible gas mixed with the fluid.

This paper mainly discusses the application of the WHAM code to various experiments performed at Stern Laboratories in Hamilton, Ontario, and at Ontario Hydro's Research Division. The former simulated a pressure tube break in a full-scale set-up. The latter simulated the overall features of the Darlington piping system in a small-scale rig.

BASIC DIFFERENTIAL EQUATIONS FOR TRANSIENT FLOW

For any flow in which viscosity (friction) cannot be ignored, complex piping systems, and so on, the propagation of pressure waves becomes very complicated, and recourse must be made to developing the basic differential equations for transient flow, and solving them with the appropriate approximations. Chief among these for the present application is that the density of water remains approximately constant (although the equations are derived for the general case of a compressible fluid). Another important assumption is that the equation of motion (momentum equation), together with the continuity equation, and the physical properties of the fluid, are sufficient to determine the wave propagation behaviour in situations where negligible heat transfer takes place, and where negligible conversion of frictional work into thermal energy takes place. These assumptions are commonly made in the modelling of acoustic phenomena in single-phase water. The change in sonic velocity with temperature change from channel inlet to outlet (e.g. during power operation) can be accounted for via the bulk modulus of the water, which is treated as a physical property of the water. The derivation of the basic differential equations for momentum and continuity are described in detail in Reference 1.

The momentum and continuity equations are a pair of quasi-linear hyperbolic partial differential equations and as such cannot easily be solved analytically. A standard method used to numerically solve systems of such wave-type equations is the "Method of Characteristics", in which the two original partial differential equations are converted to two total differential equations, each with the restriction that it is only valid along the corresponding characteristic, whose slope in space-time is given by the speed of sound. This method of numerical solution is adopted in the computer code WHAM.

At a boundary condition such as a pipe dead end, a constant pressure source, a partially open valve, and so on, there is only one characteristic available (i.e., information is transmitted at the sonic velocity either from upstream or downstream of the pipe, depending on the pipe end). As it is from the boundaries that disturbances are usually initiated, the analysis of boundary conditions is very important. The boundary conditions may take the form of some auxiliary equation that specifies either the pressure or flow, or some relation between them. This information is sufficient to determine both the pressure and flow at the boundary, in conjunction with the momentum and continuity equations.

For pipes in a complex network, the junctions between pipes constitute internal boundaries at or across which certain constraints must be imposed. Assuming no frictional losses occur at a junction, the pressure at the end of each pipe connection must be common. This is equivalent to assuming that the velocity head term may be neglected in comparison to the pressure head term (the corollory is that the energy equation may be neglected). In addition, the continuity equation must be satisfied at the junction. Thus, pressure and flow boundary conditions are imposed at each internal pipe junction, whether it be a series or a parallel connection.

NUMERICAL METHOD OF SOLUTION

Two approaches are possible to obtain a numerical solution. These are the use of a fixed space-time grid, and the use of a grid of characteristic lines. The first method offers some advantages in most fluid transient problems, since the space-time variables are assigned definite values. This is the method chosen in the WHAM model. One of the main advantages of this method is that a common fixed timestep can be used in a multi-pipe system without having to adjust other parameters.

To be assured of numerical stability, the Courant condition (also known as the CFL condition) must be met as described in Reference 1. This is achieved by the appropriate choice of Δx (axial segment length) in each pipe for a given Δt (time-step), assuming that the sonic velocity is known. Since an integral number of axial segments are also required in each pipe, this means that numerical interpolation will be the norm rather than the exception. Such Interpolations can introduce artificial numerical damping or drift into the solution, unless relatively small axial resolution is used. The WHAM code is flexible enough that extremely small resolution can be specified, without unduly slowing down the calculation time.

SONIC VELOCITY CALCULATIONS

The prediction of acoustic phenomena is strongly dependent upon the assumed sonic velocity in any segment of pipe. The sonic velocity is dependent not only upon the bulk modulus and density of the water, but also on the elastic properties of the pipe, and to a great extent, upon the amount of gas (either non-condensible such as air or nitrogen) or steam present in the water. For example, as described in Reference 1, the presence of nitrogen in the pressure/calandria tube annulus of the Stern Labs facility described below, has a strong bearing on the severity of the waterhammer transient.

An important consideration for the calculation of the sonic velocity in either the fuel channel, or the PT/CT annulus in the case of the PT rupture experiments, is that the effect of any component geometry internal to the external tube (e.g. fuel bundles) needs to be taken into account. This is done via an exact derivation of the continuity equation, which considers the cross-sectional area changes that occur due to the elastic straining of each component. This is described further in Reference 1.

In the case of the PT rupture experiments, the flow through the calandria tube is annular rather than cylindrical, since it contains a circular pressure tube. This effectively can be represented as a reduced Young's Modulus of the outer tube, when calculating the effect of wall flexibility on the sonic velocity. For nominal pressure/calandria tube dimensions the effective Young's Modulus is about 0.27 times the nominal value, i.e., a considerable reduction. This leads to a much lower sonic velocity in the calandria tube than would normally be the case for cylindrical flow in a tube.

In the case of a fuel channel, the sonic velocity is affected by the presence of the fuel bundles in a similar manner to the above. In addition, fresh or unirradiated fuel sheaths may also compress elastically, and this would further reduce the sonic velocity in the channel. In the former case (irradiated fuel), the continuity equation yields an effective PT Young's Modulus of about 0.42 times the nominal value. In the case of fresh fuel (assuming completely elastic sheathing), the continuity equation yields an effective PT Young's Modulus about 0.25 times the nominal value. Use of the effective Young's Modulus is a very convenient method of accounting for the effects of flexible piping on the sonic velocity.

Figure 1 shows the computed sonic velocity for heavy water, as a function of the water temperature at 11.4 MPa pressure. These values are used in all the WHAM reactor calculations, and similar calculations are available for light water. The computed sonic velocity is shown for feeder (steel) pipes, unirradiated and irradiated fuel channels. Also shown in the figure is the sonic velocity uncorrected for any effect of piping elasticity. It can be seen that the sonic velocity in the feeders is little affected by the elasticity of the pipe, whereas the sonic velocity in the fuel channels is significantly reduced due to elasticity effects. Channels containing unirradiated fuel have the lowest sonic velocity due to the added elastic flexibility of the sheaths.

Separate sonic velocity calculations were performed for the simulation of the PT rupture tests with WHAM, and these are described in detail in Reference 1. These tests used light water, and a nitrogen-filled PT/CT gas annulus. The large reduction of sonic velocity with a small amount of gas is important to the results of these tests, as discussed below. The effect of a small amount of void may also be important if any steam quality is present. Figure 2 shows the calculated sonic velocity as a function of the void.

THE COMPUTER CODE WHAM

As mentioned previously, the computer code WHAM was initially written to numerically solve the momentum and continuity equations for the PT rupture experiments. For this purpose, the model was set up for the general case of a network of pipes connected either in series, parallel, or a combination of both. The basic flow diagram for WHAM is discussed in Reference 1.

Later, when applying the model to the more complex geometry of an entire core pass of the Darlington reactor, major modifications were required to the WHAM code, although the basic numerical technique and solution methodology remained the same. A large effort was then devoted to setting up a more general network model, with the result that the user now has almost complete freedom to specify the desired location of junction connections (e.g., channel feeders) and branch lines (e.g., ECI/SDC piping, header ends), together with the appropriate hydraulic boundary conditions. With all these modifications, however, the WHAM code remains an essentially one-dimensional piping network transient hydraulic model.

Another important modification made to WHAM for application to Darlington, was the modelling of full coolant flow in the piping network. The user need specify only the steady-state flow in every fuel channel (e.g., obtained from NUCIRC calculations) and the model calculates the initial pressure and flow distribution along each section of piping, including the fuel channels, the reactor inlet header piping, and the pump discharge legs. The initial pressure and flow conditions are always calculated starting from the downstream end of the network. The initial distribution values are used as boundary values at time zero, and the transient solution is obtained by stepping in time using the method of characteristics. For all times greater than zero, the pressure and flow are calculated by the code, using only the fundamental equations, together with fixed pressure boundary conditions at the pump discharge outlets (cutwaters) and the reactor outlet header. Other than piping dead-ends (zero flow), and internal area/resistance changes, these are the only imposed wave reflection points for the reactor calculations.

The effect of any area change at a junction, or frictional resistance change of a pipe, orifice, venturi, or nozzle, is inherently accounted for in the solution of the acoustic wave transmission problem. All such area or resistance changes produce wave reflection, and it is important that they be accurately modelled, in such a way that the steady-state pressure drop predicted using the transient fundamental equations in the WHAM model, matches closely with that calculated by other standard codes such as NUCIRC. Equivalent friction factors are therefore derived for each pipe section, orifice, nozzle, and so on, using NUCIRC code predictions. These equivalent friction factors are then input to WHAM, with the result that transient (local) pressures and flows calculated by WHAM represent the acoustic wave transmission part, while the mean or average pressure and flow at any location are almost identical to that calculated by the NUCIRC code. This is a very useful self-check on the solution provided by WHAM, as it steps through time. Another useful self-check is that a zero wave disturbance initiated at a boundary condition should produce no change from the predicted initial pressures and flows in the piping network. That is, the solution of the transient equations following a null-disturbance should exactly equal the initial steady-state solution. This was always found to be the case with WHAM, indicating that the effect of numerical damping or drift was neglible.

In order to obtain a high degree of prediction accuracy of the changing pressure gradients, so as to determine the locations of pressure nodes and antinodes in the acoustic wave, a very small axial resolution (calculation length) of about 5 cm, or 1/10th of a fuel bundle length, was chosen for the entire 5000 metres or so of piping in a core pass. In order to satisfy the Courant criterion for numerical stability, this necessitated a calculational time step of 50 microseconds. This small time-step allows a steady-state solution to be reached relatively quickly (within about 0.5 seconds of simulation time), so that computer run time is not excessive. A typical 120 channel run on the IBM RISC computer uses about 10 Mb of core memory and takes about 3 hours.

The WHAM code, therefore, provides an extremely numerically accurate time-series solution for acoustic wave transmission in a piping network. That is, the distributed model equations themselves are solved in an accurate manner.

The required inputs to the program may be summarized as follows:

(a) all dimensions and friction/loss factors of the piping
(b) network details such as junctions, series/parallel pipe connections
(c) pressure wave velocity in each section of pipe
(d) pressure (or flow) boundary conditions as necessary
(e) steady-state flow rate through all channels
(f) logic for open/closed connections (e.g., for interconnecting pipes)
(g) calculational time step and maximum time of simulation
(h) tolerance factor on wave velocity (if applicable)
(i) input/output (I/O) instructions to the code

The outputs of the program are the pressure and flow rate at each node in each pipe of the network, as a function of time after the start of the simulation transient. All internal calculations of the program are in metres of head (pressure) and discharge flow (velocity x area), these being the two variables normally used in the analysis of fluid transients. The internal calculations are then independent of the fluid density as can be seen by inspection of the governing equations. The code uses an input fluid density only to convert the output pressure and flow to the more familiar MPa (or psi) and kgs^{-1} units.

PRESSURE TUBE RUPTURE EXPERIMENTS INVOLVING WATERHAMMER

These experiments were extensively instrumented and carefully planned, and since the observed phenomena require the solution of the same fundamental wave equations as for the acoustic phenomena, verification of WHAM against these experiments provides a measure of confidence in the methodology employed.

For application to these experiments, a simulation of the as-built loop was performed with the WHAM network model (Fig. 3). At one end of the network there is a constant pressure source (pressurizer), while at the other end a pressure/flow boundary condition is imposed to simulate the flow discharge out of the calandria tube annulus. It is the limited discharge out of the annulus which results in the deceleration of the water and the initiation of the waterhammer transient (acoustic response) in the PT/CT annulus. This deceleration follows the steam-gas-water mixing and steam void collapse sequence described in Reference 1.

The calculational time step chosen determines the number of segments in each pipe according to the Courant condition. Too large a step produces only one or two segments in the shortest pipe, while too small a step slows down the calculation time. A sensitivity study showed that a 100 ms width waterhammer pulse is accurately modelled with a 1ms time step.

Four of the most pertinent pressure tube rupture experiments were modelled with WHAM, namely Tests 1,2,5 and 6, described in detail in Reference 1. As well, numerous sensitivity analyses were conducted to assess the relative importance of various variables, and to confirm the robustness of the solution technique. These studies are also described in Reference 1.

Test 1 was the highest pressure test performed of the series, with a source (pressurizer) pressure of 11.6 MPa. The water temperature was 290 C, corresponding to a saturation pressure of about 7.5 MPa. Consequently, the pressure differential driving water to the break was about 4 MPa, and produced a high mass flow rate of about 60 kgs^{-1} into the annulus. As a result, a large peak annulus pressure was expected and a thick stainless steel calandria tube was used to contain the pressure.

Test 2 was performed at a lower source pressure (9.2 MPa) than the first test, and more importantly, at a higher temperature (300 C) corresponding to a saturation pressure of 8.6 MPa. The reduced driving pressure differential (0.6 MPa) produced a much lower initial flow rate into the annulus, so that a waterhammer effect was not expected. This test is referred to as a "low subcooling" test, in contrast with Test 1 which is referred to as a "high subcooling" test.

Test 5 was performed at 7.5 MPa and 255 C using a thinner stainless steel calandria tube than in Tests 1 and 2. Since the saturation pressure for this test is 4.3 MPa, this is termed a "high subcooling" test, with a reasonably high initial flow rate into the annulus (about 30 kgs^{-1}).

Test 6 was performed at pressure and temperature conditions very similar to Test 5. The main difference was that the calandria tube was thinner than in Test 5, and made of Zircaloy rather than steel. This tube was expected to yield at about 8.5 MPa, so the survivability of the tube was in question before the test. However, the tube did not fail but strained plastically in the hoop (i.e., circumferential) direction by a relatively large amount (0.75 percent).

Only a summary of the WHAM code predictions for the above four tests is provided here. Details may be found in Reference 1.

The four tests can be separated into two categories, namely:

(a) tests with "high" calandria tube sonic velocity (Tests 1 and 2)
(b) tests with "low" calandria tube sonic velocity (Tests 5 and 6)

Figure 4 shows a comparison of the annulus pressure transients for Tests 1 and 2. The large difference between the two tests is due mainly to the difference in inlet flow. Test 1 (with the much higher inlet flow) exhibited a much more violent waterhammer transient than Test 2. The main conclusion from this comparison is that "high" subcooling conditions result in a more severe waterhammer than "low" subcooling conditions.

Figure 5 shows a similar comparison for Tests 5 and 6. Both these tests are with "high" subcooling conditions, but the waterhammer is substantially reduced due to the low calandria tube sonic velocity resulting from plastic strain. The main conclusion from this comparison is that the greater the strain, the lower the sonic velocity, and the lower and broader the pressure pulse. Comparison of the predicted annulus pressure transients with the measured pressure transients in Figures 4 and 5 shows that the experimental results are reasonably well predicted by the WHAM model.

OHRD SMALL LOOP TESTS

A number of tests have been performed recently in the small-scale loop at OHRD, to investigate the effect of relatively simple potential design changes on the RIH acoustic response. The small loop consists of 1" diameter piping connected to the main loop in which flow is driven by a prototypical 5-vane Darlington pump. The small loop tests include the base case (no fixes), effect of pump discharge interconnect, effect of stub or branch lines, and effect of resonators of various scaled designs.

All the pertinent small loop tests have been modelled with the WHAM code at the small loop resonance temperature of 220 C. Figure 6 shows a schematic of the WHAM model for the base case. The figure also indicates the relevant modifications to simulate the other cases. In all cases, the measured amplitude and phase of the source pressure at the entrance to each simulated pump discharge line in the small loop was input to the WHAM code, and the outlet pressure near the main loop pump suction was held fixed. This ensured that the pressure drop across the small loop was equal to the pump head of the main loop. In all cases discussed below, the pressure pulse amplification is normalised to 100% at the West discharge line. Unless otherwise stated, the reference sonic velocity (corrected for pipe elasticity) used in WHAM at 220 C is held constant at 1265 m/s. Note that the uncorrected sonic velocity in light water at 220 C is calculated to be 1295 m/s.

Base Case: Figure 7 shows a comparison of the predicted vs. measured pressure pulse amplification in the two 1" discharge lines and the 1" header for the base case. Note that WHAM is able to predict the measured pressure amplification reasonably well.

3/4" Interconnect: The 3/4" interconnect case was chosen since the pressure response varies slowly with temperature at 220 C, and hence, is considered stable. This was not the case for the other interconnect cases tested (1/2" and 3/8") at this temperature. Figure 8 compares WHAM predictions with experiment for the 3/4" interconnect case. Again, relatively good agreement is obtained.

1/2 and 1/4 Wavelength Stubs: Fundamental considerations indicated that a 1/2 wavelength long stub connected near a pressure antinode on the pump discharge lines, should not reduce the RIH pressure, whereas a 1/4 wavelength stub should significantly reduce the simulated header pressure. These effects were tested in the small loop and modelled with WHAM. It is important to note that the temperature in the relatively long stub (much larger L/D ratio than the reactor case) was maintained with a small bleed flow out of the stub, and this was also modelled with WHAM.

Figure 9 compares WHAM predictions with experiment for the 1/2 wavelength (termed "lambda") case. It was found that a small change in the sonic velocity from 1265 m/s to 1275 m/s (which is well within the uncertainty normally associated with sonic phenomena) gave better agreement with the experimental data.

Figure 10 shows the corresponding results for the 1/4 wavelength test, assuming zero bleed flow through the attached stub. There is a marked decrease in the header pressure compared to the base case, but WHAM appears to overestimate the pressure reduction.

Figure 11 shows the predicted effect with WHAM, of assuming a small bleed flow through the stub, of about 0.5% of the flow in the discharge line. It can be seen that this small bleed flow has a significant effect on the results, and much better agreement is obtained with experiment when this is included. The reason for this is that zero bleed flow implies a perfect reflection boundary at the stub end, whereas a small finite bleed flow produces a lower reflection.

Resonators (Types 1 through 4): Various designs of resonator have been tested in the small loop, ranging from relatively large volume to small volume resonators, connected to the discharge lines via pipes of different diameters and lengths. The details of resonator design are not the subject of this section, and only results are shown here of the various simulations performed with WHAM compared to experimental results.

Figures 12 through 15 show the results for the four resonator cases. A striking feature of these results is that a large decrease in header pressure is obtained in all cases, and the experimental results are excellently reproduced by WHAM.

CONCLUSIONS

It is concluded that the solution technique in the one-dimensional WHAM model is more than adequate to predict the data from the full-scale pressure tube rupture experiments involving waterhammer, and the small scale tests involving acoustic pressure pulsations, with reasonable confidence.

REFERENCE

(1) "Numerical Solution of the Waterhammer Equations Using the Method of Characteristics and Comparison Against Experiments", M.Sc. Thesis by A.P. Muzumdar, Oxford University, Faculty of Mathematics, September, 1991.

FIGURE 1

SONIC VELOCITY FOR HEAVY WATER

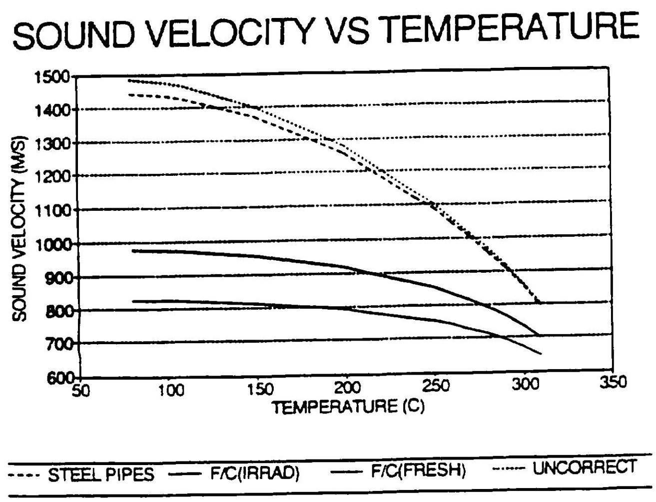

FIGURE 4

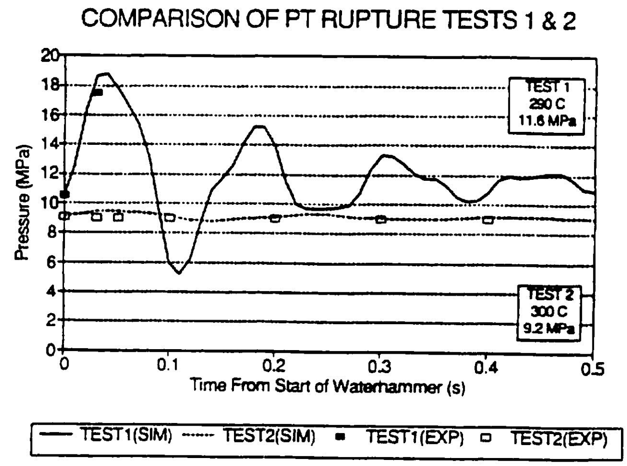

FIGURE 2

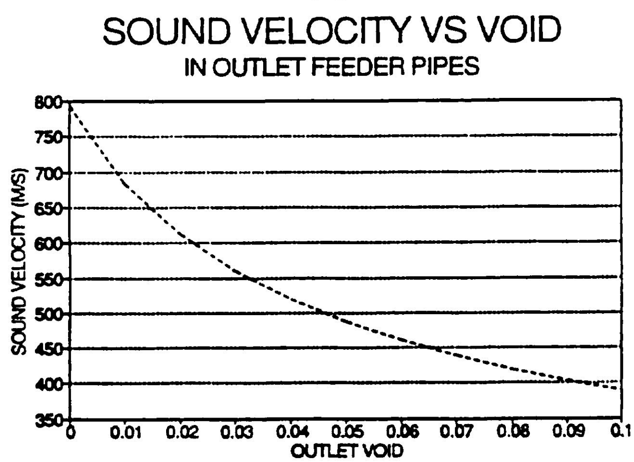

FIGURE 5

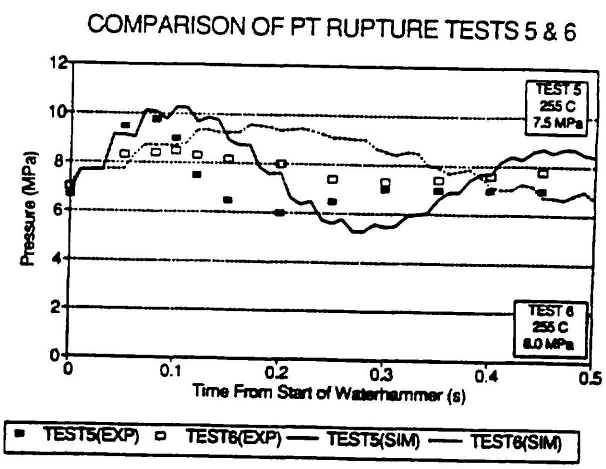

FIGURE 3

WHAM NETWORK MODEL
FOR PT RUPTURE TESTS

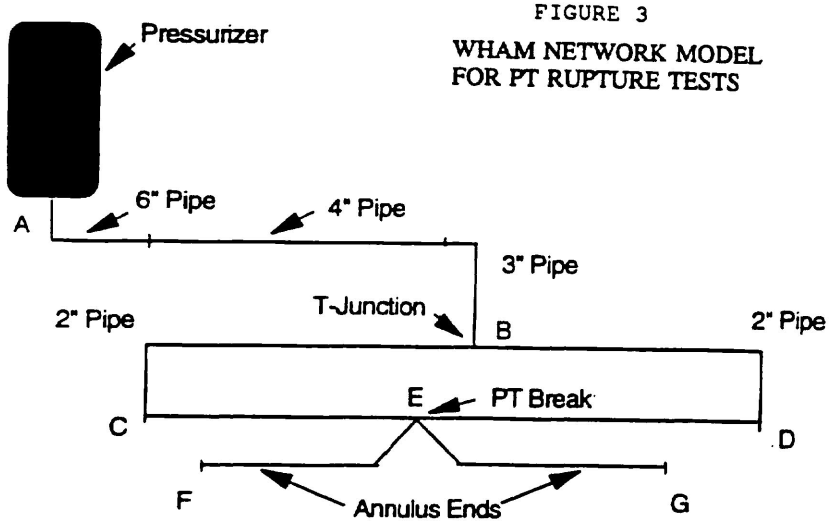

FIGURE 6

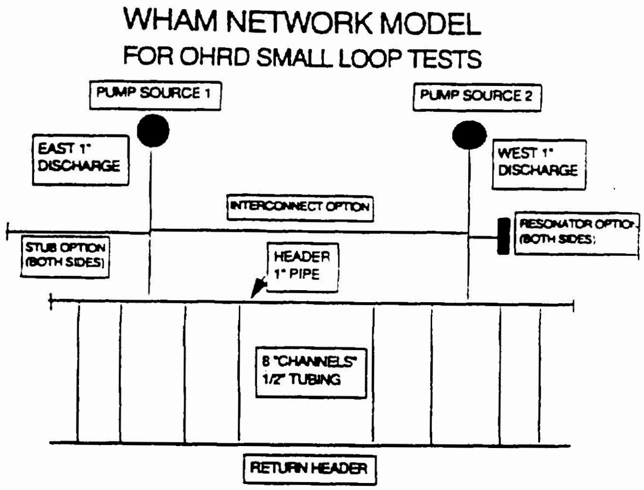

FIGURE 7

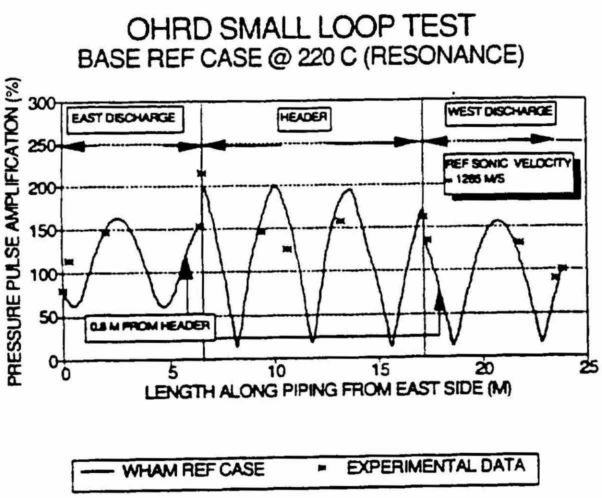

FIGURE 8

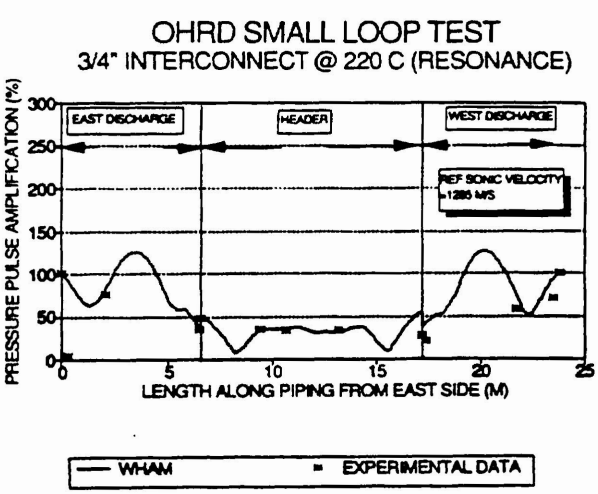

FIGURE 9

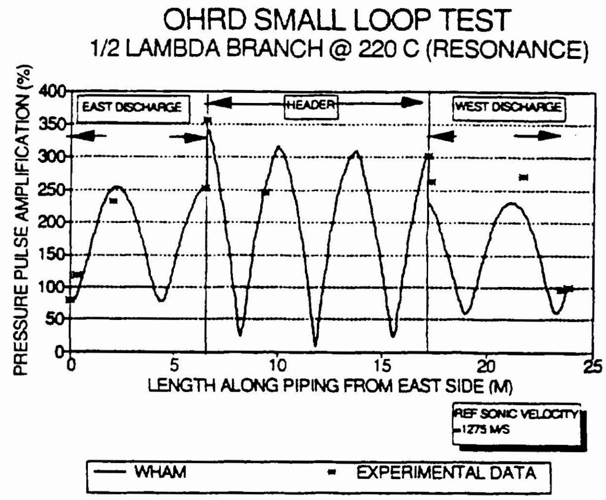

FIGURE 10

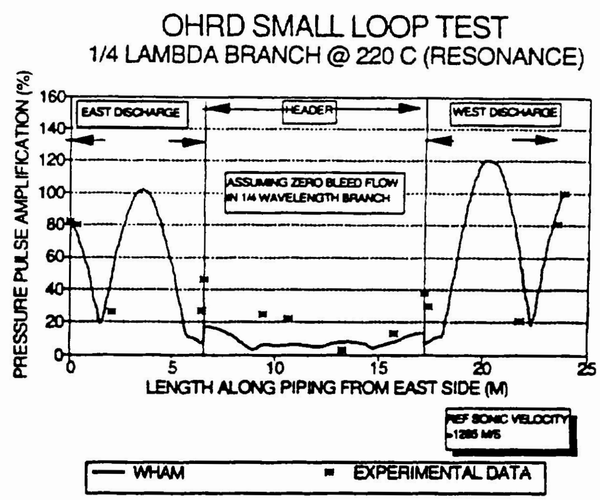

FIGURE 11

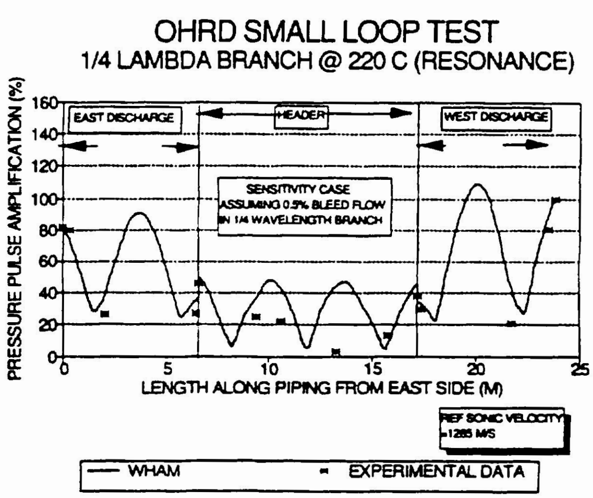

FIGURE 12

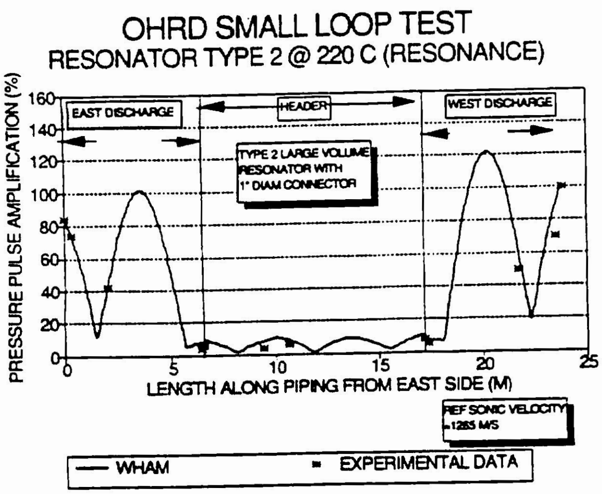

FIGURE 14

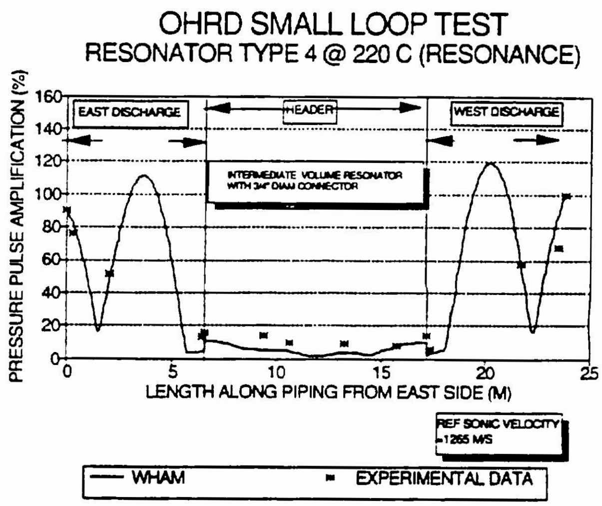

FIGURE 13

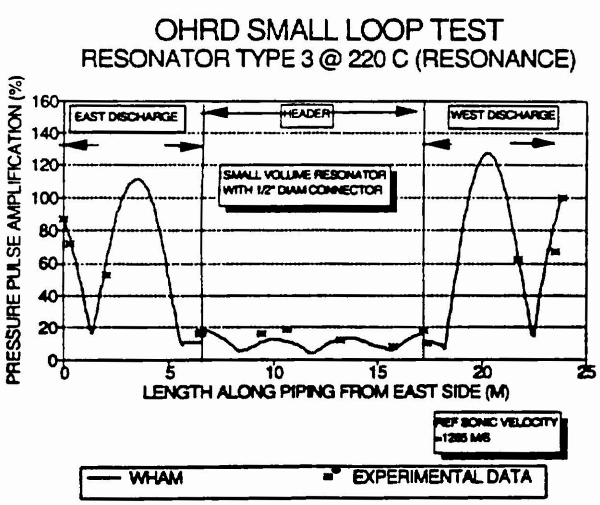

FIGURE 15